ducing the growth rates by rendering ineffective the destabilizing electron ∇B-drift resonances. Under such conditions shear stabilization of the modes appears achievable, provided the temperature gradients are not too severe. For trapped-ion instabilities, our calculations indicate that the reversed gradients should easily stabilize the modes. Here we find a strong reduction of the growth term, together with a pronounced enhancement of all damping effects. It should be pointed out, however, that ordinary dissipative and collisionless drift instabilities[3] (outside the banana regime) are further destabilized by inverted gradients. In particular, untrapped-electron resonances, which drive the unstable collisionless drift waves and also affect the trapped-electron modes,[11] can be exacerbated by such profiles. Such effects together with estimates of transport associated with the mode of operation described in the Letter are currently under investigation. As a final point, it is of interest to note that in recent studies of trapped-electron–related phenomena in the Princeton FM-1 spherator experiment, a marked reduction of unstable fluctuations was observed when oppositely directed density and temperature gradients were created.[12]

*Work supported by the U. S. Energy Research and Development Administration under Contract No. E (11-1)-3073.

[1]J. M. Dawson, H. P. Furth, and F. H. Tenney, Phys. Rev. Lett. 26, 1156 (1971); H. P. Furth and D. L. Jassby, Phys. Rev. Lett. 32, 1176 (1974).

[2]P. H. Rutherford *et al.*, to be published.

[3]B. B. Kadomtsev and O. P. Pogutse, *Reviews of Plasma Physics*, edited by M. Leontovich (Consultants Bureau, New York, 1970), Vol. 5.

[4]A. A. Galeev, in *Proceedings of the Third International Symposium on Toroidal Plasma Confinement, Garching, Germany, 26–30 March 1973*, (Max-Planck-Institut für Plasmaphysik, Garching, Germany, 1973), paper E1-I.

[5]W. Horton, Jr., *et al.*, in *Proceedings of the Fifth International Conference on Plasma Physics and Controlled Nuclear Fusion Research, Tokyo, Japan, 1974* (International Atomic Energy Agency, Vienna, Austria, 1975), paper CN-33/A14-3.

[6]J. C. Adam, W. M. Tang, and P. H. Rutherford, Princeton Plasma Physics Laboratory Report No. MATT 1156, 1975 (to be published).

[7]C. S. Liu, M. N. Rosenbluth, and W. M. Tang, Princeton Plasma Physics Laboratory Report No. MATT 1125, 1975 (to be published).

[8]W. M. Tang, P. H. Rutherford, and E. A. Frieman, to be published.

[9]The orbit-averaged curvature-drift frequency appearing here has a weak dependence on the velocity-space pitch angle ($\lambda=\mu/E$) which is ignored. This weak dependence is illustrated in Ref. 3, page 265.

[10]W. M. Tang, Phys. Fluids 17, 1249 (1974).

[11]For normal profiles, the stabilizing effect of untrapped-electron resonances on the trapped-electron modes is calculated in W. M. Tang *et al.*, Princeton Plasma Physics Laboratory Report No. MATT 1153, 1975 (to be published).

[12]S. Ejima and M. Okabayashi, Phys. Fluids 18, 904 (1975).

Magnetic Fields Due to Resonance Absorption of Laser Light*

J. J. Thomson, Claire Ellen Max, and Kent Estabrook
Lawrence Livermore Laboratory, University of California, Livermore, California 94550
(Received 2 April 1975)

We discuss the generation of dc magnetic fields due to the resonant excitation of plasma waves by an obliquely incident, plane-polarized laser beam. We show that the averaged forces on the electrons due to the plasma waves produce magnetic fields perpendicular to the plane of incidence. Megagauss field levels may be reached. Computer simulations verify our theoretical predictions.

Recently evidence has grown that megagauss magnetic fields can be generated as a result of the interaction of intense laser light with plasma.[1,2] Fields of this magnitude can have a substantial effect on the transport properties of laser-fusion plasmas.[3] Thus, it is important to understand their sources and characteristics.

Most theoretical work on this subject has concentrated on the fields due to the thermoelectric current.[1,4] In the present work, we investigate field generation that is an intrinsic part of resonance absorption. The latter process occurs when plane-polarized light is obliquely incident on a plasma with a density gradient. Since a focused laser spot contains rays with a variety of angles, resonance absorption is a ubiquitous phe-

nomenon. Moreover, its presence may be necessary for efficient light absorption.

When light is incident upon a plasma with a density gradient, its turning point is at the density $n_c \cos^2\theta$, where θ is the angle of incidence and $n_c \equiv m_e\omega^2/4\pi e^2$ is the critical density (see Fig. 1). If the laser is polarized in the plane of incidence, plasma waves are generated at n_c, where they feed energy into the plasma.[5] This dissipation introduces a phase lag between the electron oscillatory motion and the wave, causing the electrons to experience a time-averaged force. The force on the electrons determines a dc electric field (via Ohm's law) which is solenoidal for the geometry of resonance absorption. Faraday's law then gives the rate of increase of the dc magnetic field. We have seen megagauss magnetic fields in computer simulations, in agreement with our theoretical predictions.[6]

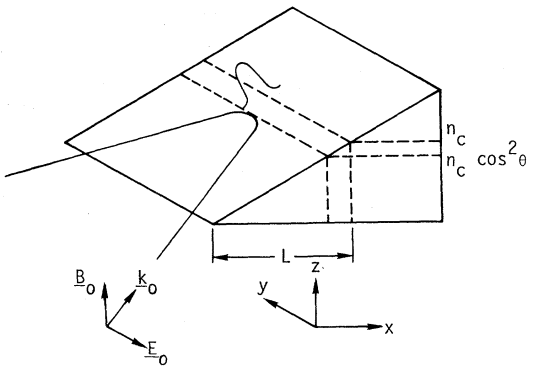

FIG. 1. Geometry for resonance absorption. Density gradient is in the x-y plane. Oscillatory and dc magnetic fields are in the z direction.

The original suggestion[7] that light absorption could produce magnetic fields did not include the effect of dissipation on the zero-order plasma dynamics, although a formal collision operator was employed. Similarly, use of the plasma electromagnetic stress tensor is not appropriate, since past derivations[8] have assumed zero absorption. Since our absorption rate is large ($\nu \sim 0.1\omega_{pe}$) and is fundamental to the field-generation process, it is necessary to include it in our lowest-order analysis. The Vlasov equation, including a simplified effective collision frequency,[9] is

$$\partial f/\partial t + \vec{v}\cdot\nabla f - (e/m_e)(\vec{E} + c^{-1}\vec{v}\times\vec{B})\cdot\partial f/\partial\vec{v} = -\nu(f - f_0). \tag{1}$$

f_0 is the Maxwellian toward which the electrons are relaxing. The mean electron density and velocity are $n \equiv \int f d^3v$, $n_0(x) \equiv \int f_0(x) d^3v$, $n\vec{V} \equiv \int \vec{v} f d^3v$.

For laser intensities of 10^{16} W/cm^2, typical of many present experiments, the high-frequency laser fields are a factor of 100 larger than the megagauss dc magnetic fields whose origin we discuss here. Consequently, the spirit of our derivation is to treat the high-frequency fields as providing the zero-order forces on the plasma. dc magnetic and electric fields are higher order in a small parameter. The dc fields will then be determined iteratively from the linear plasma response to the high-frequency fields.

In particular, we write each field quantity in terms of an oscillating and a dc part, $\vec{E} = \langle\vec{E}\rangle + \vec{E}^{\sim}$, with $\langle\vec{E}\rangle/\vec{E}^{\sim} = O(\delta) \ll 1$. The small parameter $\delta \ll 1$ is defined by $\delta \equiv eE/m_e\omega c \equiv v_0/c$, where E is the vacuum laser electric field. Our subsidiary orderings are $v_t/c \sim \nu/\omega \sim \sin\theta \sim \delta$, with $v_t \equiv (T_e/m_e)^{1/2}$. The density scale length L is ordered by $(k_0 L)^{-1} \sim \delta^2$, with $k_0 \equiv \omega/c$.

The zero-order approximation to Eq. (1) is then

$$\partial f/\partial t - (e/m_e)\vec{E}^{\sim}\cdot\partial f/\partial\vec{v} = \nu(f - f_0), \tag{2}$$

with the solution

$$f = f_0\Big(\vec{v} + (e/m_e)\int_0^t \vec{E}^{\sim}(\vec{x}, t')\,dt'\Big)e^{-\nu t} + \nu\int_0^t dt'\, e^{-\nu(t-t')} f_0\Big(\vec{v} + (e/m_e)\Big[\int_0^t \vec{E}^{\sim}(\vec{x}, t'')\,dt'' - \int_0^{t'} \vec{E}^{\sim}(\vec{x}, t'')\,dt''\Big]\Big). \tag{3}$$

Equation (3) gives the plasma response to the high-frequency fields $\vec{E}^{\sim}$. We now use this response to solve for the evolution of the dc quantities $\langle\vec{E}\rangle$ and $\langle\vec{B}\rangle$.

The velocity moment of Eq. (1) is

$$(\partial/\partial t + \nu)n\vec{V} + \nabla\cdot(n\vec{V}\vec{V}) + \nabla\cdot\Big(\int \vec{v}\vec{v} f d^3v - n\vec{V}\vec{V}\Big) = -e(n_0/m_e)\vec{E} + m_e^{-1}(\rho\vec{E} + c^{-1}\vec{J}\times\vec{B}). \tag{4}$$

We treat ions as immobile, so that $\rho \cong -e(n-n_0)$ and $\vec{J}^{\sim} = -en\vec{V}$. Equation (3) may be used to evaluate the particle pressure tensor in Eq. (4), correct to order δ^2:

$$\nabla \cdot \vec{\vec{P}}_e \equiv \nabla \cdot (\int \vec{v}\vec{v} f\, d^3v - n\vec{V}\vec{V}) = \nabla \cdot \int \vec{v}\vec{v} f_0\, d^3v\,. \tag{5}$$

We find to $O(\delta^2)$ that the time average of the electron inertia term in Eq. (4) is

$$m_e \nabla \cdot \langle n\vec{V}\vec{V}\rangle = -\nabla \cdot (1-\epsilon_R)\langle \vec{E}\vec{E}\rangle/4\pi\,. \tag{6}$$

We take $\vec{E}^{\sim} = \frac{1}{2}\{\vec{E}(x)\exp[i(\omega t - k_y y)] + \text{c.c.}\}$, and similarly for $\vec{B}^{\sim}$. ϵ_R is the real part of the complex dielectric function: $\epsilon = 1 - \omega_p^2(\omega^2+\nu^2)^{-1}(1 - i\nu/\omega)$. The time average of $\rho\vec{E} + c^{-1}\vec{J}\times\vec{B}$ is evaluated[7] by neglecting the time derivative of the Poynting vector, since the laser is a steady source. The average of Eq. (4) becomes, with use of Eqs. (5) and (6),

$$\langle \vec{E}\rangle = -(en_0)^{-1}\nabla \cdot [\tfrac{1}{2} n_0 m_e v_t^2 \vec{\vec{I}} + (8\pi)^{-1}\langle E^2 + B^2\rangle \vec{\vec{I}} - (4\pi)^{-1}\langle \epsilon_R \vec{E}\vec{E} + \vec{B}\vec{B}\rangle]\,. \tag{7}$$

The first term on the right-hand side is the thermal pressure tensor. When we take the curl of Eq. (7) to obtain $\langle \dot{\vec{B}}\rangle$, this term contributes the source for thermally generated magnetic fields, proportional to $\nabla \ln n \times \nabla T$. The second two terms in the square brackets on the right-hand side of Eq. (7) represent a generalization of the radiation pressure tensor $\vec{\vec{P}}_R$ to include absorption. For the specific example of resonance absorption, this radiation pressure is due to two effects: the average electrostatic force $(4\pi)^{-1}\langle(\nabla \cdot \vec{E})\vec{E}\rangle$ of the resonant plasma oscillations and the dc electron inertia of Eq. (6).

The curl of Eq. (7) gives the initial growth rate of $\langle \vec{B}\rangle$:

$$\partial\langle \vec{B}\rangle/\partial t = \nabla \times (c/en_0)\nabla \cdot (\vec{\vec{P}}_e + \vec{\vec{P}}_R)\,. \tag{8}$$

In a more general analysis, the right-hand side of Eq. (8) would include a diffusion term $(c^2/4\pi\sigma)\nabla^2\langle \vec{B}\rangle$, which is small in our ordering. If ions were mobile, we would add a convective term $\nabla \times (\vec{V}_i \times \langle \vec{B}\rangle)$, which could limit the growth of $\langle \vec{B}\rangle$.

We now specialize our treatment to the case of resonance absorption. Our geometry is pictured in Fig. 1. From Eq. (8), with $\nabla = \hat{x}\,\partial/\partial x$ and a linear density variation,

$$\frac{\partial\langle B_z\rangle}{\partial t} = -\frac{\partial}{\partial x}\frac{c}{en_0}\frac{\partial}{\partial x}\left[\left(1-\frac{x}{L}\right)\frac{E_x E_y^* + \text{c.c.}}{16\pi}\right]. \tag{9}$$

In the vicinity of the critical density, $x \approx L$, we use the well-known solution for the resonantly driven fields[5]:

$$E_x E_y^* + \text{c.c.} = E_0^2 \pi k_0 L \sin^2\theta \cos\theta \exp[-\tfrac{4}{3}k_0 L \sin^3\theta - (2/c)\textstyle\int_0^L \nu(x)\,dx]\,\mathrm{Re}(H_1^{(1)} H_0^{(2)})\,. \tag{10}$$

Here the argument of the Hankel functions is $(ik_0 L \sin\theta)(1 - x/L + i\nu/\omega)$. Equation (10) is strictly valid for $\sin^2\theta \gg \nu/\omega \gtrsim 1 - x/L$. We expect Eq. (10) to hold approximately for our computer simulation, in which $\sin^2\theta \gtrsim \nu/\omega$. Since damping of the electromagnetic waves is negligible except within a distance $(\nu/\omega)L$ of the critical density, $c^{-1}\int_0^L \nu(x)\,dx \cong (\nu^2/\omega^2)k_0 L$. Near n_c, Eq. (9) is approximately

$$\partial\langle B_z\rangle/\partial t = c(en_0 L^2)^{-1}(\omega/\nu)^2 (E_0^2/8\pi)\sin\theta\cos\theta\exp[-\tfrac{4}{3}k_0 L\sin^3\theta - 2k_0 L(\nu/\omega)^2]\,. \tag{11}$$

The computer simulations we discuss here used the relativistic, $2\frac{1}{2}$-dimensional particle simulation code ZOHAR.[10] Figure 1 shows the geometry. The simulation is periodic in y with no variation in z, and $\theta = 11°$. The density gradient is linear, with $L = 3\lambda_0$. Incident laser intensity is 2.2×10^{16} W/cm^2 for $\lambda_0 = 1.06$ μm, and plasma temperature is 5.1 keV.

The effective absorption rate[5] due to plasma-wave convection out of the critical region is $\nu/\omega \approx (v_t/ck_0 L)^{2/3}$, which for our parameters $(v_t/c = 0.1)$ agrees reasonably well with the value $\nu/\omega = 0.08$ observed in the simulation. We substitute the latter value into Eq. (11) and use an average for the field amplitude of $\frac{1}{2}E_{\max}{}^2$, because the resonant fields are also growing in time. Equation (11) predicts $\partial B_z/\partial t \cong 6$ MG/psec, in reasonable agreement with the observed value of 7.4 MG/psec (for Nd).

Figure 2(a) shows $\langle E_x E_y\rangle$ from the simulation, as a function of $k_0 x$. The critical density is at $k_0 x = 26$. Equation (9) indicates that $\langle \dot{B}_z\rangle > 0$ (< 0) where $\langle E_x E_y\rangle$ has positive (negative) slope. Figure 2(b) gives $\langle B_z\rangle$ as a function of $k_0 x$, showing the expected positive and negative peaks.

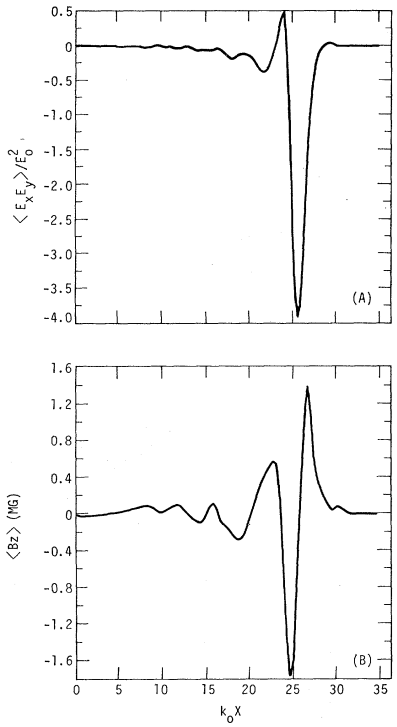

FIG. 2. Variation of $\langle E_x E_y \rangle / E_0^2$ with x, from computer simulation at time $\omega t = 162$. Parameters are described in text. E_0 is the incident laser field. (b) Resulting variation of $\langle B_z \rangle$ with x. Theory predicts $\langle \vec{B}_z \rangle \propto \partial \langle E_x E_y \rangle / \partial x$.

As the resonantly excited waves grow, they begin trapping electrons and expelling them with high velocities in the negative-x direction.[11] This gives rise to a dc current, $\langle J_x \rangle$, which can convectively limit the growth of $\langle B_z \rangle$. To account for this effect, we add the convective term $-(\partial/\partial x) \times (en_0)^{-1} \langle J_x \rangle \langle B_z \rangle$ to the right-hand side of Eq. (9). A steady state is reached when this term balances the source term, giving a maximum value for $\langle B_z \rangle$ of

$$\langle B_z \rangle = (-c/\langle J_x \rangle L)(E_x E_y^* + \text{c.c.})/16\pi . \qquad (12)$$

From the simulation, we find $\langle J_x \rangle \cong 10^{-2} en_c c$. Equation (12) then gives $\langle B_z \rangle_{max} = 3$ MG, in reasonable agreement with the observed saturation value of 1.5 MG.

In reality the ions are mobile, and nonlinear steepening of the density profile occurs.[12] This density modification alters the shape and amplitude of the resonantly excited waves. The ponderomotive force due to the resonant plasma waves forms a density depression whose lower lip can itself be above critical density. Thus, there are two surfaces where $n = n_c$, resulting in large positive peaks in $\langle B_z \rangle$ at *each* of the critical-density surfaces. We observe this effect in our simulations. On the hydrodynamic time scale, the second critical-density layer may be blown outward, leaving a single peak in $\langle B_z \rangle$ once more.

We have also investigated a computer simulation in which the light enters normally ($\theta = 0$). No resonance absorption occurs at first, and no dc magnetic field is observed. On a longer time scale, the light self-focuses and creates a "ripple" or cavity at the critical density.[13] The sides of the ripple are now oblique to the light and resonance absorption occurs, concomitant with the growth of a dc magnetic field. Megagauss fields are again observed.

The source terms in Eq. (11) extend over a width less than a Larmor radius in the gradient direction. However, in an actual experiment, the magnetic field will spread rather quickly. For example, it would take ~20 psec to diffuse resistively across 5 Larmor radii into the cold overdense region ($n_e > 10^{21}$ cm^{-3}). Once the field has spread over many Larmor radii, its effects on transport can become substantial, since cross-field values of the classical transport coefficients are reduced by the factor $(\Omega_{ce}\tau_e)^2 \sim 700$.

In conclusion, we have demonstrated that resonance absorption is accompanied by the generation of dc magnetic fields. For laser-fusion parameters, such fields may grow to megagauss levels. They can spread resistively in space sufficiently to affect seriously plasma transport properties.

We would like to thank J. Arons, J. M. Dawson, J. DeGroot, W. Kruer, B. Lasinski, A. B. Langdon, E. Valeo, and W. Woo for valuable discussions.

*Work performed under the auspices of the U. S. Energy Research and Development Administration.

[1]J. A. Stamper, K. Papadopoulous, S. O. Dean, E. A. McClean, and J. M. Dawson, Phys. Rev. Lett. 26, 1012 (1972).

[2]J. A. Stamper and B. H. Ripin, Phys. Rev. Lett. 34, 138 (1975).

[3]J. B. Chase, J. M. LeBlanc, and J. R. Wilson, Phys. Fluids 16, 1142 (1973); G. H. Dahlbacka, Bull. Am. Phys. Soc. 18, 1340 (1973); N. K. Winsor and D. A. Tidman, Phys. Rev. Lett. 31, 1044 (1973).

[4]D. A. Tidman and R. A. Shanny, Phys. Fluids 17, 1207 (1974).

[5]V. L. Ginzburg, *Propagation of Electromagnetic*

Waves in Plasmas (Pergamon, New York, 1970), Sect. 20; J. P. Friedberg, R. W. Mitchell, R. L. Morse, and L. I. Rudsinski, Phys. Rev. Lett. 28, 795 (1972).

[6]Megagauss magnetic fields were first identified as due to resonance absorption in computer simulations by A. B. Langdon and B. F. Lasinski (private communication). D. W. Forslund and E. L. Lindman have also observed dc magnetic fields in simulations (private communication).

[7]J. A. Stamper and D. A. Tidman, Phys. Fluids 16, 2024 (1973).

[8]L. D. Landau and E. M. Lifshitz, *Electrodynamics of Continuous Media* (Pergamon, New York, 1960), p. 256; L. P. Pitaevskii, Zh. Eksp. Teor. Fiz. 39, 1450 (1960) [Sov. Phys. JETP 12, 1008 (1961)].

[9]N. A. Krall and A. W. Trivelpiece, *Principles of Plasma Physics* (McGraw-Hill, New York, 1973), pp. 315–317.

[10]A. B. Langdon and B. F. Lasinski, in "Methods in Computational Physics," edited by J. Killeen *et al.* (Academic, New York, to be published), Vol. 16.

[11]K. G. Estabrook, E. J. Valeo, and W. L. Kruer, "Two-Dimensional Relativistic Simulations of Resonance Absorption" (to be published), Figs. 2 and 3.

[12]K. G. Estabrook, E. J. Valeo, and W. L. Kruer, Phys. Lett. 49A, 109 (1974).

[13]E. J. Valeo and K. G. Estabrook, Phys. Rev. Lett. 34, 1008 (1975).

Electromagnetic Ion-Beam Instabilities in the Solar Wind*

Michael D. Montgomery, S. Peter Gary, D. W. Forslund, and W. C. Feldman
Los Alamos Scientific Laboratory, University of California, Los Alamos, New Mexico 87544
(Received 14 May 1975)

The stability of a plasma consisting of two, unequal, isotropic, ion beams streaming along a uniform magnetic field has been investigated by numerically solving the full electromagnetic, Vlasov, linear dispersion relation for high-β plasmas. Three instabilities are found: One is closely associated with the usual Alfvén mode and the two others with the "fast" or magnetosonic mode. The importance of these instabilities for certain neutral-beam-injection experiments and in the solar wind is emphasized.

Recent IMP-6 solar-wind observations[1,2] have shown the regular appearance of persistent, double-peaked, ion-velocity distributions. The two peaks are generally unequal in size, are often clearly resolved, and may be separated by as much as the local Alfvén speed C_A parallel to the ambient magnetic field $\vec{B}_0$. Since $\beta = 8\pi nT/B_0^2$ is moderately high, it is appropriate to utilize the complete electromagnetic dispersion relation. For this study the range $0.05 \leq \beta \leq 1$ is considered. This range is also of interest for future neutral-beam-heating experiments in moderately dense plasmas.[3]

Theoretical investigation of electromagnetic ion-beam instabilities effectively began with Stepanov and Kitsenko.[4] They concluded that both right- and left-hand circularly polarized modes (commonly termed magnetosonic and Alfvén waves, respectively) propagating parallel to $\vec{B}_0$ could be driven unstable by a weak, secondary ion beam also directed along $\vec{B}_0$. However, these results are subject to question because they calculated growth rates from frequencies which did not include either the particle thermal velocities or contributions due to the beam. Later work[5,6] has used the same questionable technique.

More recently, growth rates for ion-beam velocities much greater than the Alfvén speed C_A have been calculated,[7] and the special case of propagation perpendicular to the ambient magnetic field for equal-density components has been treated.[8] Growth rates for obliquely propagating electrostatic ion-cyclotron waves in a warm plasma have also been evaluated.[9]

This Letter presents selected results from a more general investigation of electromagnetic ion-beam instabilities carried out by numerically solving the electromagnetic, Vlasov, linear dispersion relation for a homogeneous plasma including off-angle propagation.[10] These results represent substantial improvements over those obtained with use of the cold-plasma approximation.

For this study, a three-component plasma configuration is assumed, consisting of a main proton component (hereafter denoted by the subscript M), a counterstreaming (in the center-of-mass frame), secondary proton component (beam) denoted by the subscript B, and an electron component e, where each component is assumed to be an isotropic Maxwellian. The plasma is electrically neutral, $n_M + n_B = n_e$, and bears no current, $n_M V_{0M} + n_B V_{0B} = 0$ and $V_{0e} = 0$. The V_{0j} are the drift velocities of the various $(j = M, B, e)$